ELSEVIER

Neurobiology of Aging 33 (2012) 488–498

NEUROBIOLOGY OF AGING

www.elsevier.com/locate/neuaging

Microstructural changes and atrophy in brain white matter tracts with aging

Stefania Sala[a], Federica Agosta[a], Elisabetta Pagani[a], Massimiliano Copetti[b], Giancarlo Comi[c], Massimo Filippi[a,c,*]

[a] *Neuroimaging Research Unit, Institute of Experimental Neurology, Division of Neuroscience, Scientific Institute and University Ospedale San Raffaele, Milan, Italy*

[b] *Biostatistics Unit, IRCCS-Ospedale Casa Sollievo della Sofferenza, Foggia, Italy*

[c] *Department of Neurology, Scientific Institute and University Ospedale San Raffaele, Milan, Italy*

Received 12 January 2010; received in revised form 31 March 2010; accepted 19 April 2010

Abstract

Diffusion tensor (DT) magnetic resonance imaging (MRI) tractography was used to investigate microstructural and volumetric abnormalities of the major brain white matter (WM) tracts with aging in 84 healthy subjects. Linear relationships were found between age and mean diffusivity (MD) increase and fractional anisotropy (FA) decrease in all WM tracts, except the right cingulum and bilateral uncinate, where a linear correlation with age was found for FA only. Quadratic model fitted better MD and FA values of several tracts, including the corpus callosum, limbic pathways, and bilateral association, and corticospinal tracts. Age-related MD and FA abnormalities were associated with radial diffusivity increase in all WM tracts, while axial diffusivity changes were characterized by a considerable variation from a tract to another. A linear negative relationship with age was found for the volumes of the left cingulum and fornix, while the quadratic model fitted better age-related volume loss of corpus callosum and right inferior fronto-occipital fasciculus. Diffusion tensor magnetic resonance imaging may shed light into the complex pathological substrates of WM changes with aging.

Keywords: Aging; White matter tracts; Diffusion tensor MRI; Tractography; Atrophy

1. Introduction

Early diffusion tensor (DT) magnetic resonance imaging (MRI) studies of normal aging focused on 2 indexes (Madden et al., 2009a): mean diffusivity (MD), which is the average of the 3 eigenvalues of the DT and measures the magnitude of water molecule diffusion, and fractional anisotropy (FA), which is defined as a coefficient of variation of the eigenvalues and is an index of the degree of directionality of water diffusivity (Basser et al., 1994; Pierpaoli et al., 1996). However, the assessment of individual eigenvalues is likely to contribute to a better understanding of the pathological substrates associated with aging (Bennett et al., 2009; Burzynska et al., 2009; Davis et al., 2009; Madden et al., 2009b; Sullivan et al., 2010; Vernooij et al., 2008; Zahr et al., 2009; Zhang et al., 2008). The first eigenvalue is called axial diffusivity (diffusion parallel to the axon fibers; AD), whereas the second and third eigenvalues can be averaged and expressed as radial diffusivity (diffusivity perpendicular to the axonal fibers; RD) (Basser et al., 1994; Pierpaoli et al., 1996). Axonal damage, as occurs in secondary degeneration, is likely to result in decreased AD values (Pierpaoli et al., 2001), while myelin breakdown is associated with an increased RD and a normal AD (Pierpaoli et al., 2001; Song et al., 2002, 2003). More recently, a

* Corresponding author at: Neuroimaging Research Unit, INSPE, Scientific Institute and University, Ospedale San Raffaele, via Olgettina 60, 20132 Milan, Italy. Tel.: +39 02 26433033; fax: +39 02 26435972.
E-mail address: massimo.filippi@hsr.it (M. Filippi).

0197-4580/$ – see front matter © 2012 Elsevier Inc. All rights reserved.
doi:10.1016/j.neurobiolaging.2010.04.027

method to obtain estimates of white matter (WM) fiber bundle volumes using DT MRI has been developed (Pagani et al., 2007). This approach provides an index of atrophy derived from the transformation between an FA atlas (resuming average morphometry of a reference population) and individual subjects' FA maps (Pagani et al., 2007).

The assessment of the extent of age-related intrinsic changes and volume loss of specific WM pathways is likely to be more informative than that of global WM involvement (Johansen-Berg and Behrens, 2006). The location of WM abnormalities can be inferred from the analysis of regions of interest, voxel-wise comparisons, or projecting diffusion values onto a tract-based template (Madden et al., 2009a). All these approaches, however, make assumptions on the anatomy of the damaged WM tracts. An alternative strategy is to use DT MRI tractography to segment individual WM tracts (Johansen-Berg and Behrens, 2006). To date, only a few studies used quantitative DT MRI tractography to test the effect of aging on brain WM structures (Davis et al., 2009; Fjell et al., 2008; Madden et al., 2009b; Sullivan et al., 2010; Zahr et al., 2009), and only 1 tractography study reported AD and RD values of all the main cerebral WM tracts in adults between 20 and 81 years (Sullivan et al., 2010). The effect of age on DT MRI metrics (i.e., increased MD and decreased FA) varied from a fiber bundle to another, and was associated consistently with an increase in RD values in most WM tracts (Sullivan et al., 2010), thus suggesting demyelination as the most likely substrate of age-related WM abnormalities (Pierpaoli et al., 2001; Song et al., 2002, 2003). The volume loss of specific WM pathways with aging has never been assessed.

In this study, we investigated comprehensively the microstructural and volumetric abnormalities of the major inter- and intrahemispheric WM tracts with aging, using DT MRI tractography, in a large sample of healthy subjects spanning from the adolescence to the adult age range. Fiber bundles examined were the corpus callosum, limbic pathways (i.e., fornix and cingulum), major bilateral association tracts (i.e., uncinate, inferior fronto-occipital [IFO], inferior longitudinal [ILF], and superior longitudinal [SLF] fasciculi), and corticospinal tract (CST). Our main aims were to assess whether: (1) aging has an effect on different structural brain WM measures, such as diffusivity properties and regional atrophy; (2) the effect of age on WM tract abnormalities, if any, is linear or nonlinear; and (3) there is a relationship between microstructural and volumetric age-related abnormalities within each WM tract. We hypothesized that WM tracts would differ with respect to age-related changes in diffusivity properties and volume (Burzynska et al., 2009). In particular, we expected that the interhemispheric, limbic, and frontal association pathways would be the most damaged with aging. On the basis of cross-sectional (Bartzokis et al., 2001; Bartzokis, 2004; Courchesne et al., 2000; Jernigan et al., 2001) and longitudinal (Raz et al., 2005) studies showing that WM integrity and volume continue to increase into middle ages, remain relatively stable up to age of 40 to 50 years, and then undergo a steep decline, we also predicted that the quadratic function would improve the relations of diffusivity and volumetric age-related changes in most of the WM tracts. Another central question is whether WM diffusivity changes are independent of the corresponding fiber bundle atrophy (Fjell et al., 2008; Hugenschmidt et al., 2008). Diffusivity changes are related to several aspects of the WM microstructure, some of which are likely to also affect volume, e.g., degree of myelination and axonal degeneration (Basser et al., 1994; Pierpaoli et al., 1996). However, it is also expected that diffusivity metrics may be early markers of loss of tissue integrity that only at a later stage will be detectable by volumetric WM measures (Fjell et al., 2008; Hugenschmidt et al., 2008).

2. Methods

2.1. Subjects

Subjects were recruited by means of advertisements distributed in the community. All subjects were assessed clinically by an experienced neurologist. Participants were excluded if they had: (1) a history of major neurological, psychiatric, or cardiovascular diseases, or any other major systemic condition; (2) a history of alcohol or drug abuse; (3) an abnormal neurological examination; and (4) a WM hyperintensity (WMH) grade greater than 2 at the Wahlung rating scale score (Wahlund et al., 2001). Eight-four healthy volunteers (48 women and 36 men, mean age 44 years, range 13–70 years) were enrolled. Eighty-one subjects (96.4%) were right-handers and 3 subjects (3.6%) left-handers according to the 10-item version of the Edinburgh Handedness Inventory Scale (Oldfield, 1971). The main demographic characteristics of the subjects in each age group have been reported elsewhere (Pagani et al., 2008). Approval was received from the local ethical standards committee on human experimentation and written informed consent was obtained from all subjects participating in the study.

2.2. MRI data acquisition

Using a 1.5-T scanner (Avanto, Siemens, Erlangen, Germany), the following scans of the brain were obtained: (1) dual-echo (DE) turbo spin echo (SE), and (2) pulsed-gradient spin echo single shot echo-planar (PGSE-SS-EPI). Further details regarding the magnetic resonance (MR) acquisition protocol are reported elsewhere (Pagani et al., 2008).

2.3. MRI data analysis

All MRI analysis was performed by a single experienced observer, blinded to subjects' identity. WMHs, if any, were identified on dual-echo scans, and the WMH loads measured using a local thresholding segmentation technique

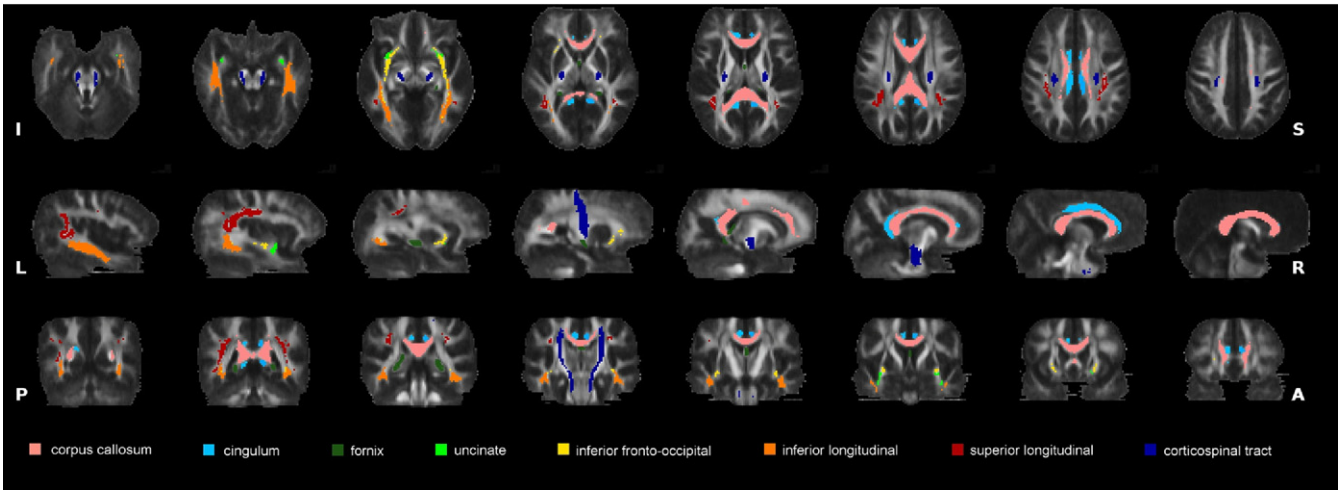

Fig. 1. White matter tract probability maps obtained from the reference healthy subjects. Probability maps are superimposed on axial (top row), sagittal (middle row), and coronal (bottom row) sections of the fractional anisotropy atlas. A, anterior; I, inferior; L, left; P, posterior; R, right; S, superior.

(Rovaris et al., 1997). An atlas-based automated approach was used to obtain DT MRI-derived metrics of the brain WM tracts. This procedure involved: (1) the creation of a reference FA image in the standard space (the FA atlas) using the data from the group of healthy subjects ranging from 21 to 40 years of age (reference group; 24 subjects, 15 women and 8 men, mean age 29 years); (2) the definition of WM tract probability maps on the FA atlas (Fig. 1); (3) the nonlinear alignment of individual subjects' MD, FA, AD, and RD maps to the FA atlas, as well as the determinant of the Jacobian (JD) of the transformation; and (4) the application of the WM tract probability maps to the individual subject's images to measure mean tract MD, FA, AD, RD, and JD. Values for the subgroup of subjects with WMHs, lesion probability maps (LPM) of T2-visible lesions were produced, and the spatial distribution of lesions according to WM tract location was assessed. The details of MRI data analysis are described in the supplementary data e1.

2.4. Statistical analysis

The relationships between subjects' age and DT MRI metrics of the WM tracts were assessed using linear and quadratic regression models. The goodness of the fit of linear and nonlinear models was assessed by the adjusted R^2 coefficient. Results are given as β regression coefficients. Then, DT MRI metrics of each WM tract entered multivariate linear regression models where the subject's age was the dependent variable. A multivariate model stepwise selection using Akaike Information Criterion (AIC) starting from the full model was used, i.e., starting from the model with all covariates and then deleting 1 covariate at each step, until minimum Akaike Information Criterion was reached. In addition, because multivariate analysis does not account for nonlinear relationships and may be affected by correction for multiple comparisons, a random forest approach for regression analysis was also used (Breiman, 2001). This approach models simultaneously the relationship between an outcome (i.e., subject's age) and multiple potential predictor variables (i.e., diffusivity and volumetric variables), and provides us with information on variable importance. Such an analysis was performed for DT MRI metrics of each WM tract, separately. According to the random forest technique (Breiman, 2001), 100,000 trees were built. The training set used to grow each tree is a .632+ bootstrap resample of the observations (Efron and Tibshirani, 1997). The best split at each node was selected from a random subset of covariates. The left-out observations (i.e., "out of bag" observations) were then predicted to obtain the mean squared error (MSE) of the considered tree. The goodness of the fit of the random forest was assessed averaging the single tree MSE. Furthermore, the random forest framework estimates the importance of a predictor by looking at how much MSE increases when out of bag data for that variable is permuted while all others are left unchanged. The variables' importance was reported as a ranking: each covariate gets a score according to its ability to predict correctly the dependent variable (i.e., subject's age) according to the increase of MSE when values of that covariate in a node are randomly permuted. A p value < 0.05 was considered as significant. All analyses were performed with R (language and environment for statistical analysis, version 2.10.1). For the random forest analysis we used the package "randomForest" version 4.5 implemented in R (*www.r-project.org*).

3. Results

3.1. Conventional MRI

As reported previously (Pagani et al., 2008), 31 subjects (37%) had 1 or more small, nonspecific WMHs on the

Table 1
Correlation coefficients, regression coefficients and p values of the relationships of white matter tract mean diffusivity and fractional anisotropy values with age

WM tract	Side	MD								FA							
		Linear			Quadratic					Linear			Quadratic				
		R^2	β	p	R^2	β_1	p_1	β_2	p_2	R^2	β	p	R^2	β_1	p_1	β_2	p_2
CC	—	0.15	0.72	< 0.001	0.25	−2.69	0.01	0.04	0.001	0.24	−0.64	<0.001	0.28	0.80	0.27	−0.02	0.04
Cingulum	R	0.02	0.22	0.17	0.12	−2.33	0.01	0.03	0.004	0.13	−0.51	0.001	0.16	0.69	0.41	−0.01	0.15
	L	0.06	0.34	0.03	0.16	−2.42	0.01	0.03	0.002	0.29	−0.67	< 0.001	0.29	−0.09	0.90	−0.01	0.39
Fornix	—	0.24	7.15	< 0.001	0.29	−11.30	0.16	0.22	0.02	0.37	−1.83	< 0.001	0.42	1.91	0.20	−0.04	0.01
Uncinate	R	0.01	0.16	0.33	0.06	−1.73	0.07	0.02	0.04	0.19	−0.70	< 0.001	0.21	0.43	0.64	−0.01	0.21
	L	0.05	0.36	0.05	0.07	−1.01	0.35	0.02	0.19	0.07	−0.42	0.01	0.09	0.99	0.31	−0.02	0.15
Inferior fronto-	R	0.17	0.63	< 0.001	0.19	−0.42	0.64	0.01	0.24	0.19	−0.75	< 0.001	0.21	0.57	0.57	−0.02	0.18
occipital	L	0.14	0.56	< 0.001	0.16	−0.37	0.68	0.01	0.29	0.15	−0.58	< 0.001	0.15	−0.06	0.95	−0.01	0.56
Inferior	R	0.14	0.63	< 0.001	0.18	−1.19	0.22	0.02	0.06	0.38	−0.74	< 0.001	0.40	0.17	0.78	−0.01	0.13
longitudinal	L	0.11	0.56	0.002	0.15	−1.18	0.23	0.02	0.77	0.42	−0.81	< 0.001	0.45	0.38	0.53	−0.01	0.048
Superior	R	0.11	0.54	0.002	0.12	−0.15	0.88	0.01	0.48	0.28	−0.94	< 0.001	0.31	0.68	0.48	−0.02	0.09
longitudinal	L	0.15	0.60	< 0.001	0.23	−1.96	0.03	0.03	0.004	0.34	−0.90	< 0.001	0.35	0.14	0.86	−0.01	0.19
Corticospinal	R	0.19	0.48	< 0.001	0.27	−1.34	0.03	0.02	0.003	0.37	−0.75	< 0.001	0.37	−0.52	0.41	−0.01	0.72
	L	0.16	0.48	< 0.001	0.26	−1.73	0.01	0.03	0.001	0.34	−0.79	< 0.001	0.35	−1.09	0.13	0.01	0.67

Key: β, linear regression coefficient; β_1, linear component regression coefficient; β_2, quadratic component regression coefficient; CC, corpus callosum; FA, fractional anisotropy; L, left; MD, mean diffusivity; p, statistical significance of the linear regression coefficient; p_1, statistical significance of the linear component regression coefficient; p_2, statistical significance of the quadratic component regression coefficient; R, right; R^2, percentage of variance explained by the model; WM, white matter.

T2-weighted MRI scans. Mean WMH loads per each age year decade are reported elsewhere (Pagani et al., 2008).

3.2. MD and FA values of the WM tracts

Table 1 shows the correlation coefficients, regression coefficients and p values of the relationships of WM tract MD and FA values with age. A positive linear correlation was found between subject age and MD in all WM tracts, bilaterally (R^2 values ranged from 0.24 to 0.05), except for the right cingulum and bilateral uncinate fasciculus (Figs. 2 and 3). In all WM tracts, a negative linear correlation was found between subject age and FA (R^2 values ranged from 0.42 to 0.07) (Figs. 2 and 3). The quadratic regression model fitted better MD increase with age (U-shaped curve) in the corpus callosum, left cingulum, fornix, left SLF, and CST bilaterally (R^2 values ranged from 0.29 to 0.16), and FA decrease with age (inverted U-shaped curve) in the corpus callosum, fornix, and left ILF (R^2 values ranged from 0.45 to 0.28) (Figs. 2 and 3). MD increase in the right cingulum ($R^2 = 0.12$) and uncinate ($R^2 = 0.06$) correlated with age only when using the quadratic model (U-shaped curve) (Figs. 2 and 3).

3.3. AD and RD values of the WM tracts

Table 2 shows correlation coefficients, regression coefficients and p values of the relationships of WM tract AD and RD values with age. A linear positive correlation was found between subject age and AD in the fornix ($R^2 = 0.23$) (Fig. 2). The right uncinate ($R^2 = 0.08$) and SLF ($R^2 = 0.03$) AD values were correlated negatively with age (Fig. 3). The quadratic model (U-shaped curve) fitted better AD changes with age in the corpus callosum, left cingulum, left SLF, and CST bilaterally (R^2 values ranged from 0.22 to 0.04) (Figs. 2 and 3). A linear positive correlation was found between subject age and RD in Allee WM tracts (R^2 values ranged from 0.36 to 0.08) (Figs. 2 and 3). The quadratic model (U-shaped curve) fitted better RD increase with age in the corpus callosum, cingulum bilaterally, fornix, left ILF, and SLF bilaterally (R^2 values ranged from 0.33 to 0.16) (Figs. 2 and 3).

3.4. Volumes of the WM tracts

A linear negative correlation was found between subject age and WM tract volumes in the left cingulum ($R^2 = 0.12$, regression coefficient [β] = −1.78, $p = 0.001$) and fornix ($R^2 = 0.15$, $\beta = -2.19$, $p < 0.001$) (Fig. 4). A linear positive correlation was found between age and volume of the right IFO fasciculus ($R^2 = 0.08$, $\beta = 1.60$, $p = 0.01$); however, the quadratic regression model (inverted U-shaped curve) fitted better volume loss with age in this tract ($R^2 = 0.13$, $\beta_1 = 8.90$, $p_1 = 0.01$, $\beta_2 = -0.09$, $p_2 = 0.03$) (Fig. 4). The volume loss of the corpus callosum correlated with age only when using the quadratic model ($R^2 = 0.10$, $\beta_1 = 7.04$, $p_1 = 0.004$, $\beta_2 = -0.08$, $p_2 = 0.004$) (Fig. 4). No correlation was found between subject age and volumes of the remaining WM tracts.

3.5. Variable importance: multivariate and random forest analyses

Table 3 shows the results of the multivariate linear regression analysis for each WM tract. For each variable retained by the multivariate model, regression's coefficient and adjusted R^2 are reported. Multivariate models retained

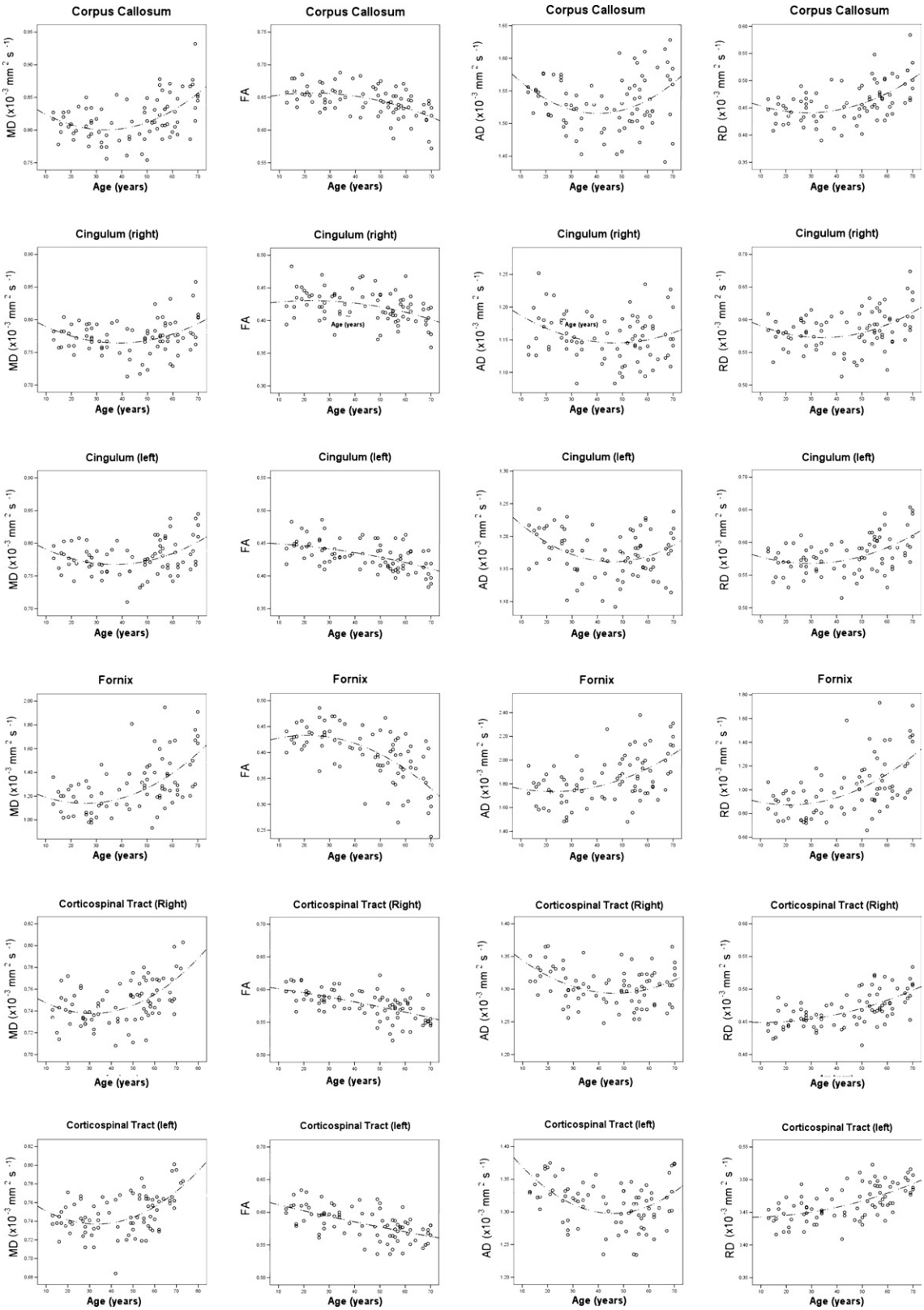

Fig. 2. Regression plots between age and diffusion tensor (DT) magnetic resonance imaging (MRI) metrics (i.e., mean diffusivity [MD], fractional anisotropy [FA], axial diffusivity [AD], and radial diffusivity [RD]) for the linear (continuous line) and quadratic (dotted line) models used to assess the corpus callosum, limbic pathways (i.e., fornix and cingulum), and corticospinal tract (CST) changes.

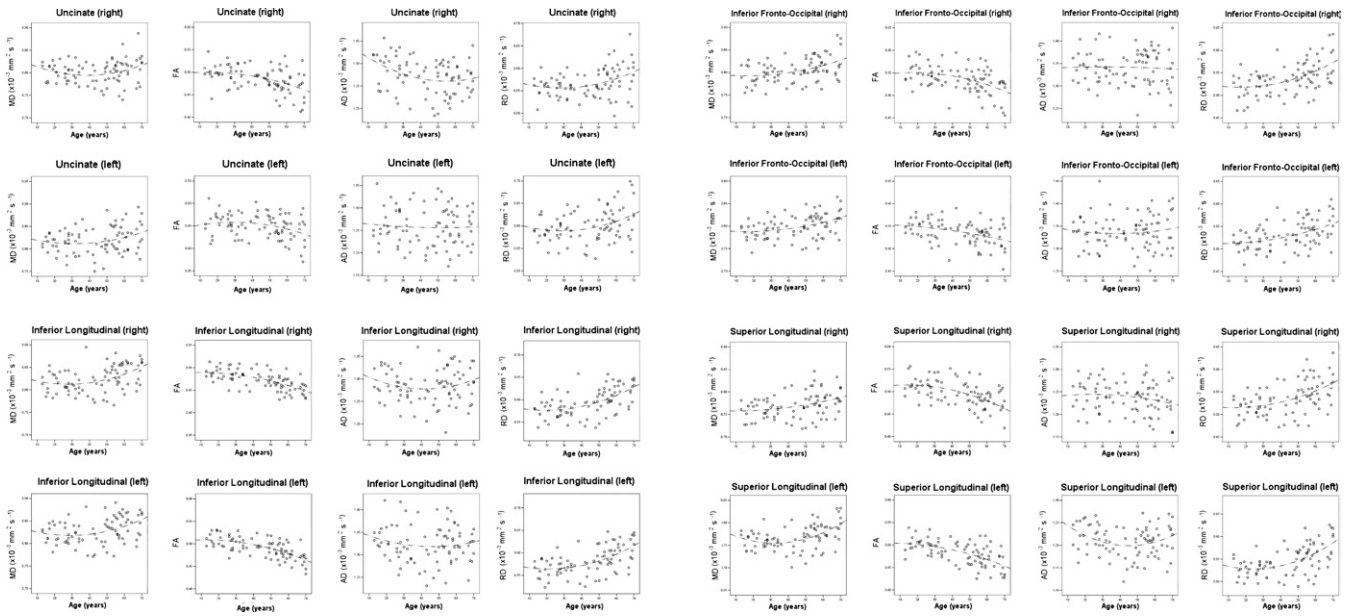

Fig. 3. Regression plots between age and diffusion tensor (DT) magnetic resonance imaging (MRI) metrics (i.e., mean diffusivity [MD], fractional anisotropy [FA], axial diffusivity [AD], and radial diffusivity [RD]) for the linear (continuous line) and quadratic (dotted line) models used to assess the major bilateral association tracts (i.e., uncinate, inferior fronto-occipital [IFO], inferior longitudinal [ILF], and superior longitudinal [SLF] fasciculi) changes.

diffusivity abnormalities and volume loss as independent predictors of subject's age in the fornix, uncinate, IFO fasciculus, and ILF (Table 3). In the corpus callosum, cingulum, SLF, and CST, only diffusivity changes were independently associated with age (Table 3). Table 3 also reports the results of the random forest analysis. For each WM tract, the proportion of explained variance estimated by the random forest analysis, as well as the rankings of DT MRI variables in terms of importance in predicting correctly subject's age are provided. The ranking of variables importance showed that, for the majority of the WM tracts, FA and RD were the most important predictors of subject's age. Volume loss was among the best predictors of subject's age in the fornix and IFO fasciculus.

3.6. WMH spatial distribution according to WM tracts

Fig. 5 shows T2 LPM in the 31 subjects with WMHs. The total number of lesional voxels belonging to all WM

Table 2
Correlation coefficients, regression coefficients and p values of the relationships of white matter tract axial and radial diffusivities with age

WM tract	Side	AD								RD							
		Linear			Quadratic					Linear			Quadratic				
		R^2	β	p	R^2	β_1	p_1	β_2	p_2	R^2	β	p	R^2	β_1	p_1	β_2	p_2
CC	—	0.01	0.18	0.49	0.10	−3.96	0.006	0.05	0.004	0.24	0.99	< 0.001	0.31	−2.01	0.07	0.04	0.01
Cingulum	R	0.02	−0.31	0.17	0.07	−2.72	0.04	0.03	0.06	0.08	0.48	0.01	0.16	−2.12	0.03	0.03	0.01
	L	0.03	−0.32	0.14	0.14	−4.07	0.001	0.04	0.002	0.17	0.67	< 0.001	0.24	−1.61	0.08	0.03	0.01
Fornix	—	0.23	5.50	< 0.001	0.27	−6.75	0.29	0.15	0.053	0.29	7.28	< 0.001	0.33	−8.10	0.26	0.18	0.03
Uncinate	R	0.08	−0.66	0.01	0.11	−2.75	0.05	0.03	0.13	0.10	0.57	0.004	0.13	−1.19	0.28	0.02	0.11
	L	0.001	−0.09	0.75	0.002	−4.51	0.78	0.004	0.82	0.08	0.59	0.01	0.11	−1.26	0.32	0.02	0.14
Inferior fronto-	R	0.001	−0.07	0.77	0.002	0.19	0.89	−0.003	0.85	0.24	0.99	< 0.001	0.27	−0.72	0.52	0.02	0.12
occipital	L	0.002	0.10	0.68	0.01	−0.77	0.58	0.01	0.53	0.20	0.79	< 0.001	0.21	−0.18	0.86	0.01	0.34
Inferior	R	0.00	0.02	0.94	0.03	−2.06	0.15	0.03	0.14	0.28	0.92	< 0.001	0.31	−0.76	0.41	0.02	0.07
longitudinal	L	0.004	−0.15	0.56	0.02	−1.61	0.30	0.02	0.34	0.28	0.92	< 0.001	0.32	−0.95	0.31	0.02	0.04
Superior	R	0.03	−0.37	0.01	0.04	0.72	0.58	−0.01	0.39	0.23	0.99	< 0.001	0.25	−0.58	0.62	0.02	0.02
longitudinal	L	0.01	−0.20	0.35	0.08	−3.24	0.01	0.04	0.01	0.28	1.00	< 0.001	0.32	−1.35	0.19	0.03	0.02
Corticospinal	R	0.04	−0.32	0.07	0.16	−3.50	0.001	0.04	0.001	0.36	0.88	< 0.001	0.38	−0.35	0.66	0.01	0.11
	L	0.04	−0.38	0.08	0.22	−5.18	< 0.001	0.06	< 0.001	0.35	0.90	< 0.001	0.36	−0.01	0.99	0.01	0.25

Key: β, linear regression coefficient; β_1, linear component regression coefficient; β_2, quadratic component regression coefficient; CC, corpus callosum; FA, fractional anisotropy; L, left; MD, mean diffusivity; p, statistical significance of the linear regression coefficient; p_1, statistical significance of the linear component regression coefficient; p_2, statistical significance of the quadratic component regression coefficient; R, right; R^2, percentage of variance explained by the model; WM, white matter.

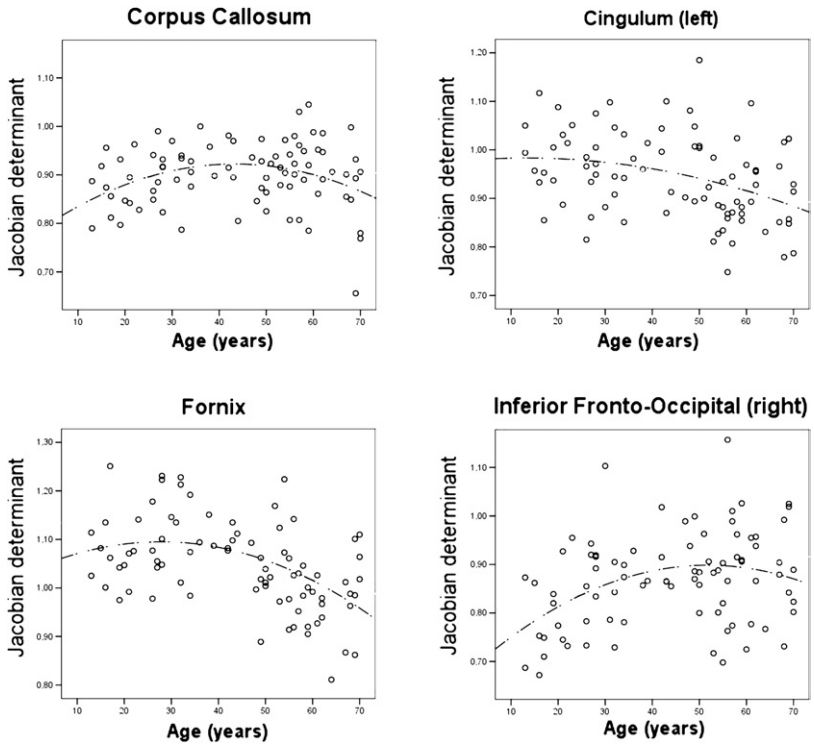

Fig. 4. Regression plots between age and the Jacobian determinants of volume changes for the linear (continuous line) and quadratic (dotted line) models used to assess the corpus callosum, left cingulum, fornix, and right inferior fronto-occipital fasciculus.

tracts studied was 858 (9.9% of the total WMH load). The spatial correspondence between T2 lesions and WM tracts ranged from 0% in the right cingulum, fornix, and left uncinate to 2.1% in the left SLF (Fig. 5).

4. Discussion

The majority of previous DT MRI studies of normal aging have investigated differences in WM diffusivity properties comparing small samples of young and old adults. Clearly, this precludes to assess potential nonlinearities in WM structural differences in the intermediate age groups. In addition, there is still a limited knowledge about the patterns of different structural brain WM measures, such as diffusivity abnormalities and regional atrophy. In this study, we investigated microstructural and volumetric age-related changes in the major WM tracts of the brain using DT MRI tractography in a relatively large group of healthy subjects spanning 6 decades of life. Linear and nonlinear relationships between aging and different diffusivity and volumetric parameters were explored. We found age-related MD increases and FA decreases in the majority of WM tracts studied, which were associated with increased RD values and AD changes that varied from a tract to another. WM tracts with a significant volume loss with aging were only the corpus callosum, limbic pathways (i.e., cingulum and fornix), and right IFO fasciculus. These diffusivity and volumetric abnormalities may reflect different phases of the "cascade of degeneration" (Burzynska et al., 2009) involving the brain WM with aging.

4.1. MD and FA abnormalities of WM tracts

The significant relationships found between age and MD increases and FA decreases of most of the WM tracts studied fit with postmortem investigations (Aboitiz et al., 1996; Meier-Ruge et al., 1992), which revealed degradation of WM microstructure with age, including an increase of brain water content, demyelination, disruption of axon structure, and overall rarefaction of fibers. The linear models showed that WM integrity decreases from the second to the seventh decade of life in the CST and interhemispheric, limbic, and frontal association pathways. As it has been speculated in numerous studies (see for instance Sullivan et al., 2010), this pattern of abnormalities agrees with the notion that subtle damage to the frontal and limbic systems may contribute to age-related decline of cognitive and motor functions. The nonlinear functions improved the relation between MD increases with age in most of the WM tracts, as well as that between age and FA decrease in the corpus callosum, fornix, and ILF. The inclusion of adolescents, coupled with the comparison between linear and quadratic fittings, allowed us to collect evidence that aging of the WM is characterized by a considerable variation from a tract to another and that part of this variation is likely to be related to maturational aspects of the different fiber bundles (Giorgio et al., 2010).

Table 3
Variables' importance as derived by the random forest analysis and multivariate linear regression analysis

WM tract	Random forest analysis		Multivariate analysis		
	Explained variance (%)	Variable importance	β	p	Adjusted R^2
CC	83.4	FA	2.02	0.001	0.36
		RD	6.71	0.02	
		MD	−7.40	0.07	
		AD	1.94	0.15	
		volume	—	—	
Cingulum	73.4	L FA	−0.57	< 0.001	0.29
		L RD	—	—	
		L AD	−0.07	0.15	
		L MD	—	—	
		R MD	—	—	
		R FA	0.17	0.14	
		R RD	—	—	
		L volume	—	—	
		R AD	—	—	
		R volume	—	—	
Fornix	70.1	FA	−0.18	< 0.001	0.42
		Volume	−0.01	0.004	
		RD	—	—	
		MD	—	—	
		AD	—	—	
Uncinate	74.9	R FA	—	—	0.39
		R AD	—	—	
		R RD	0.56	<0.001	
		R MD	−0.59	<0.001	
		R volume	0.05	<0.001	
		L volume	0.02	0.04	
		L MD	0.59	0.07	
		L RD	—	—	
		L FA	0.43	0.13	
		L AD	−0.28	0.15	
Inferior fronto-occipital	76.1	L volume	0.06	0.006	0.48
		R RD	—	—	
		L RD	—	—	
		R volume	0.03	0.17	
		R MD	0.95	0.02	
		R FA	0.53	0.11	
		L FA	0.83	0.09	
		L MD	1.24	0.04	
		R AD	−0.48	0.03	
		L AD	−0.71	0.03	
Inferior longitudinal	67.1	L FA	−0.53	< 0.001	0.42
		R FA	—	—	
		L RD	—	—	
		R RD	—	—	
		R MD	—	—	
		L MD	—		
		R AD	—	—	
		L AD	—	—	
		R volume	—	—	
		L volume	0.03	0.13	
Superior longitudinal	76.2	L RD	—	—	0.37
		L FA	−0.32	< 0.001	
		R FA	—	—	
		L MD	—	—	
		R RD	0.27	0.02	
		R MD	−0.32	0.01	
		R AD	—	—	
		L AD	—	—	
		L volume	—	—	
		R volume	—	—	
Corticospinal	67.9	L FA	0.75	0.05	0.42
		L RD	—	—	
		R RD	0.23	0.05	
		L AD	−0.67	0.01	
		R FA	—	—	
		R MD	—	—	
		L MD	1.21	0.02	
		R volume	—	—	
		R AD	—	—	
		L volume	—	—	

Key: AD, axial diffusivity; CC, corpus callosum; FA, fractional anisotropy; L, left; MD, mean diffusivity; R, right; RD, radial diffusivity; WM, white matter.

4.2. AD and RD abnormalities of WM tracts

In line with previous reports (Bennett et al., 2009; Burzynska et al., 2009; Davis et al., 2009; Madden et al., 2009b; Zahr et al., 2009; Zhang et al., 2008), increased MD and decreased FA values with age were found to be associated with an increase of RD values in all WM tracts. It is usually assumed that RD is modulated by the extracellular distance between membranes, axon diameter, and degree of myelination (Pierpaoli et al., 2001). As a consequence, our findings suggest that such structural abnormalities possibly underlying age-related RD changes affect WM microstructure throughout the whole brain. Conversely, we found that the behavior of AD values with age was more variable. AD values were found (1) to linearly decrease with age in the right uncinate and SLF; (2) to linearly increase with age in the fornix; (3) to have a U-shaped relationship with age in the corpus callosum, left cingulum, and SLF, as well as CST bilaterally; and (4) not to undergo detectable changes in the remaining WM tracts. The dissociation between RD (a possible marker of myelination) and AD (a possible marker of axonal integrity) (Pierpaoli et al., 2001) suggests that age-related differences in MD and FA values are likely to be driven mostly by myelodegeneration (Pierpaoli et al., 2001; Song et al., 2002, 2003; Sotak, 2002). This agrees with histopathological findings of an age-related loss of myelin and myelinated fibers in elderly people (Aboitiz et al., 1996; Meier-Ruge et al., 1992; Terao et al., 1994).

Nevertheless, we cannot exclude that axonal degeneration also plays a role in the observed diffusivity abnormalities. Indeed, in vivo axonal degeneration is characterized by a series of events which make challenging the interpretation of AD abnormalities in normal adults with different ages. Our findings suggest that the different age-related RD/AD patterns that we observed may reflect a variable severity of the same underlying pathological process rather

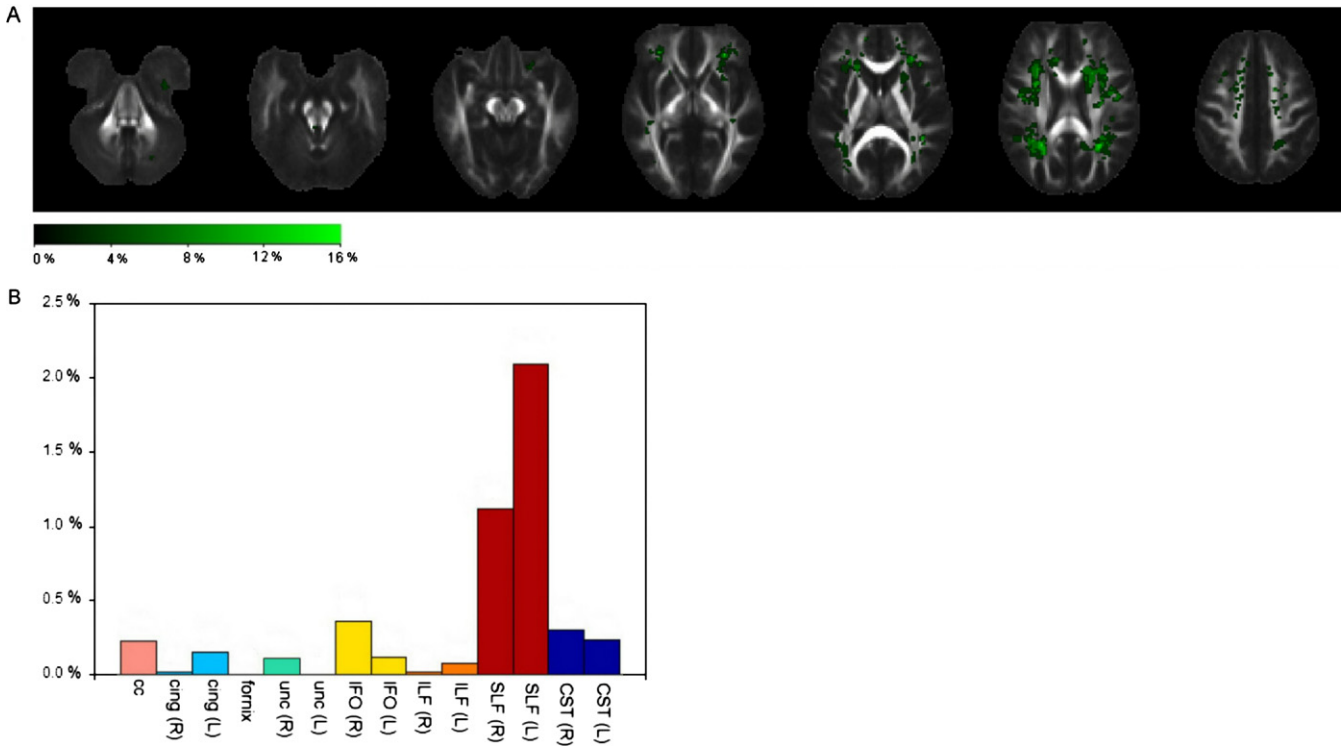

Fig. 5. (A) T2 lesion probability map (LPM) from the 31 healthy subjects with white matter (WM) hyperintensities. In the T2 LPM, voxel intensity indicates how frequently a voxel is part of a lesion across all subjects. (B) The graph shows the percentage of each WM tract involved by lesional voxels.

than potentially diverse characteristics of the aging WM (Bennett et al., 2009; Burzynska et al., 2009). AD changes have been observed to follow a biphasic pattern after acute brain injury (Concha et al., 2006). For instance, soon after the transection of the corpus callosum in epileptic subjects, a decrease of AD values has been observed (Concha et al., 2006), which may be due to the break-up of axons into small fragments creating barriers to the longitudinal displacement of water molecules. The cellular debris is subsequently cleared by microglia, allowing the water molecules to once again diffuse parallel to the surviving axons, which may result in a normalization or even an increase of AD (Concha et al., 2006). Albeit aging is clearly not an acute event, this biphasic process may be helpful in the interpretation of our DT MRI data. At the time of scanning, WM fibers may in fact experience variable degrees of AD changes secondary to the relative extents of neuronal loss and cellular debris clearance (Burzynska et al., 2009). In our study, the inclusion of intermediate age groups and the use of nonlinear regression analysis allowed to gain some insight into the "cascade of degeneration" that may occur with aging. For instance, we disclosed a U-shaped pattern of age-related AD changes in the corpus callosum (a weak decrease until the age of 40 years, a steadiness in the 40–50-year decade, and an increase by the age of 50), which would have gone undetected if data would have been analyzed only with a linear regression model.

4.3. Volume loss of the WM tracts and its relationship with DT MRI changes

An additional novelty of the present study is that we used DT MRI data to explore another potential marker of WM damage with age, namely the size of fiber bundles. Compared with diffusivity changes, the pattern of volume loss was more restricted and included only the corpus callosum, limbic network, and right IFO fasciculus. It is worth noting that the behavior of WM volume changes would have been misinterpreted by simply using a linear regression analysis. The quadratic fitting showed that the volumes of the corpus callosum and IFO fasciculus increase until the 40–50-year decade and then decrease at a relatively rapid pace. It is also of interest to note that only some of the fiber bundles with intrinsic damage (i.e., increased MD and decreased FA values) also experienced volume loss.

The multivariate and random forest analyses allowed us to gain additional insight into the relationship between diffusivity and volumetric WM properties. Multivariate models showed that diffusivity abnormalities and volume loss were independently associated with aging in some of the WM tracts, such as the fornix, uncinate, IFO fasciculus, and ILF. On the other hand, in the corpus callosum, cingulum, SLF, and CST, diffusivity changes were more sensitive than volumes to changes in WM integrity with aging. There are at least 2 possible explanations, which are not mutually

exclusive, for this topographical mismatch. First, diffusivity metrics may be sensitive to pathological changes which do not influence individual tract volumes. Second, diffusivity abnormalities may precede WM atrophy in some of the brain WM tracts. The random forest analysis provided several important pieces of information from this dataset in addition to the "classical" statistical analysis. Indeed, the random forest analysis showed an extremely high performance of DT MRI variables in predicting subject's age in all WM tracts. Not surprisingly, compared with other WM tracts, the corpus callosum explained most of the age effect. The corpus callosum is the major neural system of WM tracts in the brain and functions as the principal conduit of interhemispheric communication. Postmortem studies of the corpus callosum indicates significant age-related structural increase during development to adulthood (Yakovlev and Lecours, 1967) and deterioration, including breakdown of myelin and microtubules and deletion of small diameter fibers, with senescence (Aboitiz et al., 1996; Pandya and Seltzer, 1986). Our findings are in line with previous MRI reports showing in vivo that corpus callosum fibers, mainly in the anterior regions, are particularly vulnerable to aging (Bartzokis, 2004; Ota et al., 2006; Sullivan et al., 2002, 2006, 2010). Functional meaningfulness of these age-related differences was supported by the findings of a significant correlation between MRI signs of corpus callosum degradation and poorer performance on cognitive and motor tests (Sullivan et al., 2006, 2010; Zahr et al., 2009). The random forest analysis also defined a list of variables' importance, which can contribute to define better the relationship between aging and the different MRI quantities. For the majority of the WM tracts studied, FA and RD were the most important predictors of subject's age, while volume loss was among the best predictors of subject's age in the fornix and IFO fasciculus, only. Taken together with previous observations (Fjell et al., 2008; Hugenschmidt et al., 2008), our findings suggest that diffusivity measures detect microstructural changes in WM before atrophy as well as in atrophied tissue.

4.4. Contribution of WMHs to age-related DT MRI abnormalities

Subjects with significant vascular pathology on conventional MRI scans were not included in the present study and nonspecific WMHs were found in 31 subjects. The analysis of the spatial distribution of WMHs showed that only 9.9% of the WM tracts studied was involved by lesional voxels. Clearly, we cannot rule out that subtle ischemic disease may have an impact on the observed WM DT MRI changes. Indeed, chronic ischemia might contribute with myelin degeneration in increasing RD values (Pierpaoli et al., 2001; Song et al., 2002, 2003; Sotak, 2002). On the contrary, the combination of vascular pathology and axon degeneration would most likely result in the opposite effect on AD (increasing and reducing AD values, respectively), thus possibly causing an AD "pseudonormalization".

4.5. Limitations and conclusions

Some limitations of our study ought to be mentioned. First, we do not have histopathological data on our subjects and, therefore, we can only speculate on the possible pathological substrates underlying the observed DT MRI changes. However, such data are not easy to be obtained, especially in the younger subject population, unless many years have passed between MRI and histopathology, which would inevitably make challenging the interpretation of DT MRI abnormalities. Second, the current study is cross-sectional. Third, both univariate and multivariate analyses were reported for each WM. However, due to the high intercorrelation between DT MRI metrics, results from the univariate models should be taken with caution. Finally, some methodological problems related to DT MRI should be considered. Regions of crossing fibers are characterized by a low anisotropy and, thus, the determination of fiber orientation may be difficult in these areas (Henry et al., 2003). However, the fasciculi that we investigated are all major WM tracts with high anisotropy values, and, therefore, diffusivity changes due to crossing fibers should not have affected our results a great deal (Henry et al., 2003). In addition, because the information used to make inference on WM tract size was based on FA, we cannot rule out completely that some WM tracts might have been wrongly considered atrophic, while they might simply harbor intrinsic microstructural changes. Finally, cortical and WM atrophic changes may cause partial volume effects from the cerebrospinal fluid in DT MR images and consequently increase the probability of false positive findings. In our analysis, precautions were taken to ensure that this may not have influenced the results a great deal and contamination from the CSF was minimized by deriving DT MRI-based metrics from WM tracts after WM map thresholding. Despite these limitations, our study demonstrates that different patterns of microstructural and volumetric abnormalities occur with aging in brain WM tracts from healthy subjects, and contributes to shed light into the complex pathological substrates of such age-related changes.

Disclosure statement

S. Sala, F. Agosta, E. Pagani and M. Copetti report no disclosures. G. Comi reports consulting services: Bayer Schering Pharma, Serono Symposia International Foundation, Merck Serono, Teva Pharmaceutical Industries, Ltd, and Biogen-Dompé AG; speaking activities: Teva Pharmaceutical Industries, Ltd, Sanofi-Aventis, Serono Symposia International Foundation, Biogen-Dompé AG, and Bayer Schering Pharma. M. Filippi reports scientific advisory boards: Teva Pharmaceutical Industries, Ltd and Genmab, A/S; funding for travel: Bayer Schering Pharma, Biogen-

Dompé AG, Genmab, A/S, Merck Serono, and Teva Pharmaceutical Industries, Ltd.; editorial boards: American Journal of Neuroradiology, BMC musculoskeletal Disorders, Clinical Neurology and Neurosurgery, Erciyes Medical Journal, Lancet Neurology, Magnetic Resonance Imaging, Multiple Sclerosis, and Neurological Sciences; consultant: Bayer Schering Pharma, Biogen-Dompé AG, Genmab, A/S, Merck Serono, and Teva Pharmaceutical Industries, Ltd.; speakers' bureaus: Bayer Schering Pharma, Biogen-Dompé AG, Genmab, A/S, Merck Serono, Teva Pharmaceutical Industries, Ltd.; research support: Bayer-Schering, Biogen-Dompé AG, Genmab, A/S, Merck Serono, Teva Pharmaceutical Industries, Ltd, Fondazione Italiana Sclerosi Multipla (FISM), and Fondazione Mariani.

Approval was received from the local ethical standards committee on human experimentation and written informed consent was obtained from all subjects participating in the study.

Supplementary data e1

MRI data analysis

a. Diffusion tensor preprocessing

Diffusion tensor (DT) analysis was carried out using an in-house software. Diffusion weighted images were first corrected for distortion induced by eddy currents (Studholme et al., 1997), then the DT was estimated by a linear regression (Basser et al., 1994), and mean diffusivity (MD), fractional anisotropy (FA), axial diffusivity (AD) and radial diffusivity (RD) maps computed (Basser and Pierpaoli, 1996).

b. FA atlas creation

The FA atlas was obtained using DT magnetic resonance imaging (MRI) images using the data from the group of healthy subjects ranging from 21 to 40 years of age (reference group; 24 subjects, 15 women and 8 men, mean age = 29 years), as previously described (Pagani et al., 2008). Briefly, their dual-echo scans were registered to the standard Montreal Neurological Institute (MNI) space (Mazziotta et al., 2001) with affine transformation using the VTK CISG Registration Toolkit (Studholme et al., 1997). This transformation was then applied to FA images to correct for differences in head size between subjects. Subsequently, FA maps were nonlinearly transformed with an iterative procedure to produce an average shape and intensity image atlas (Pagani et al., 2008).

c. WM tract probability maps

On the reference FA maps, fiber tracking (Pagani et al., 2005) was performed to segment the major brain white matter (WM) tracts, bilaterally. These included: corpus callosum, fornix, cingulum, uncinate fasciculus, inferior fronto-occipital fasciculus, inferior longitudinal fasciculus, superior longitudinal fasciculus, and corticospinal tract. Single subject's WM tracts were registered to the atlas space, using the transformation matrices previously computed, and averaged to produce WM tract probability maps. These maps were then thresholded at 40%. WM tract probability maps are shown in Fig. 1.

d. DT MRI metrics of the WM tracts

The nonlinear transformation between the FA atlas and the FA maps of each subject was estimated (Rohde et al., 2003), as well as the determinant of the Jacobian (JD) of the transformation (Pagani et al., 2007). This scalar index summarizes the point-wise volume changes produced by the deformation: values less than unity reflect atrophy, whereas values greater than unity reflect hypertrophy (Pagani et al., 2007). The nonlinear transformation was then applied to each subject's MD, FA, AD and RD, as well as to JD maps. WM tract probability maps were used as masks and average MD, FA, AD, RD, and JD values of each tract measured.

e. Spatial distribution of WMHs

For the subgroup of subjects with white matter hyperintensities (WMHs), T2 lesion probability maps (LPM) were created and normalized to the Montreal Neurological Institute (MNI) space using the transformation matrices previously calculated. In the T2 LPM, voxel intensity indicates how frequently a voxel is part of a lesion across all subjects with WMHs (Fig. 5). The spatial distribution of T2 lesions according to WM tract location was then assessed by applying the T2 LPM on WM tract probability maps and the percentage of each WM tract involved by lesional voxels computed.

References

Aboitiz, F., Rodriguez, E., Olivares, R., Zaidel, E., 1996. Age-related changes in fibre composition of the human corpus callosum: sex differences. Neuroreport 7, 1761–1764.

Bartzokis, G., 2004. Age-related myelin breakdown: a developmental model of cognitive decline and Alzheimer's disease. Neurobiol. Aging 25, 5–18.

Bartzokis, G., Beckson, M., Lu, P.H., Nuechterlein, K.H., Edwards, N., Mintz, J., 2001. Age-related changes in frontal and temporal lobe volumes in men: a magnetic resonance imaging study. Arch. Gen. Psychiatry 58, 461–465.

Basser, P.J., Mattiello, J., leBihan, D., 1994. Estimation of the effective self-diffusion tensor from the NMR spin echo. J. Magn. Reson. B 103, 247–254.

Bennett, I.J., Madden, D.J., Vaidya, C.J., Howard, D.V., Howard, J.H., Jr., 2009. Age-related differences in multiple measures of white matter integrity: A diffusion tensor imaging study of healthy aging. Hum. Brain Mapp. 31, 378–390.

Breiman, L., 2001. Random forests. Mach. Learn. 45, 5–32.

Burzynska, A.Z., Preuschhof, C., Backman, L., Nyberg, L., Li, S.C., Lindenberger, U., Heekeren, H.R., 2009. Age-related differences in white matter microstructure: Region-specific patterns of diffusivity. Neuroimage 49, 2104–2112.

Concha, L., Gross, D.W., Wheatley, B.M., Beaulieu, C., 2006. Diffusion tensor imaging of time-dependent axonal and myelin degradation after corpus callosotomy in epilepsy patients. Neuroimage 32, 1090–1099.

Courchesne, E., Chisum, H.J., Townsend, J., Cowles, A., Covington, J., Egaas, B., Harwood, M., Hinds, S., Press, G.A., 2000. Normal brain development and aging: quantitative analysis at in vivo MR imaging in healthy volunteers. Radiology 216, 672–682.

Davis, S.W., Dennis, N.A., Buchler, N.G., White, L.E., Madden, D.J., Cabeza, R., 2009. Assessing the effects of age on long white matter tracts using diffusion tensor tractography. Neuroimage 46, 530–541.

Efron, B., Tibshirani, R.J., 1997. Improvements on cross-validation: the .632+ bootstrap method. J. Am. Stat. Assoc. 92, 548–560.

Fjell, A.M., Westlye, L.T., Greve, D.N., Fischl, B., Benner, T., van der Kouwe, A.J., Salat, D., Bjornerud, A., Due-Tonnessen, P., Walhovd, K.B., 2008. The relationship between diffusion tensor imaging and volumetry as measures of white matter properties. Neuroimage 42, 1654–1668.

Giorgio, A., Watkins, K.E., Chadwick, M., James, S., Winmill, L., Douaud, G., De Stefano, N., Matthews, P.M., Smith, S.M., Johansen-Berg, H., James, A.C., 2010. 1. Longitudinal changes in grey and white matter during adolescence. Neuroimage 49, 94–103.

Henry, R.G., Oh, J., Nelson, S.J., Pelletier, D., 2003. Directional diffusion in relapsing-remitting multiple sclerosis: a possible in vivo signature of Wallerian degeneration. J. Magn. Reson. Imaging 18, 420–426.

Hugenschmidt, C.E., Peiffer, A.M., Kraft, R.A., Casanova, R., Deibler, A.R., Burdette, J.H., Maldjian, J.A., Laurienti, P.J., 2008. Relating imaging indices of white matter integrity and volume in healthy older adults. Cereb. Cortex 18, 433–442.

Jernigan, T.L., Archibald, S.L., Fennema-Notestine, C., Gamst, A.C., Stout, J.C., Bonner, J., Hesselink, J.R., 2001. Effects of age on tissues and regions of the cerebrum and cerebellum. Neurobiol. Aging 22, 581–594.

Johansen-Berg, H., Behrens, T.E., 2006. Just pretty pictures? What diffusion tractography can add in clinical neuroscience. Curr. Opin. Neurol. 19, 379–385.

Madden, D.J., Bennett, I.J., Song, A.W., 2009a. Cerebral white matter integrity and cognitive aging: contributions from diffusion tensor imaging. Neuropsychol. Rev. 19, 415–435.

Madden, D.J., Spaniol, J., Costello, M.C., Bucur, B., White, L.E., Cabeza, R., Davis, S.W., Dennis, N.A., Provenzale, J.M., Huettel, S.A., 2009b. Cerebral white matter integrity mediates adult age differences in cognitive performance. J. Cogn. Neurosci. 21, 289–302.

Meier-Ruge, W., Ulrich, J., Bruhlmann, M., Meier, E., 1992. Age-related white matter atrophy in the human brain. Ann. N.Y. Acad. Sci. 673, 260–269.

Oldfield, R.C., 1971. The assessment and analysis of handedness: the Edinburgh inventory. Neuropsychologia 9, 97–113.

Ota, M., Obata, T., Akine, Y., Ito, H., Ikehira, H., Asada, T., Suhara, T., 2006. Age-related degeneration of corpus callosum measured with diffusion tensor imaging. Neuroimage 31, 1445–1452.

Pagani, E., Agosta, F., Rocca, M.A., Caputo, D., Filippi, M., 2008. Voxel-based analysis derived from fractional anisotropy images of white matter volume changes with aging. Neuroimage 41, 657–667.

Pagani, E., Horsfield, M.A., Rocca, M.A., Filippi, M., 2007. Assessing atrophy of the major white matter fiber bundles of the brain from diffusion tensor MRI data. Magn. Reson. Med. 58, 527–534.

Pandya, D.N., Seltzer, B., 1986. The topography of commissural fibers, in: Lepore, F., Ptito, M., Jasper, H.H. (Eds.), Two Hemispheres − One Brain: Functions of the Corpus Callosum. Alan R. Liss, New York, pp. 47–74.

Pierpaoli, C., Barnett, A., Pajevic, S., Chen, R., Penix, L.R., Virta, A., Basser, P., 2001. Water diffusion changes in Wallerian degeneration and their dependence on white matter architecture. Neuroimage 13, 1174–1185.

Pierpaoli, C., Jezzard, P., Basser, P.J., Barnett, A., Di Chiro, G., 1996. Diffusion tensor MR imaging of the human brain. Radiology 201, 637–648.

Raz, N., Lindenberger, U., Rodrigue, K.M., Kennedy, K.M., Head, D., Williamson, A., Dahle, C., Gerstorf, D., Acker, J.D., 2005. Regional brain changes in aging healthy adults: general trends, individual differences and modifiers. Cereb. Cortex 15, 1676–1689.

Rovaris, M., Filippi, M., Calori, G., Rodegher, M., Campi, A., Colombo, B., Comi, G., 1997. Intra-observer reproducibility in measuring new putative MR markers of demyelination and axonal loss in multiple sclerosis: a comparison with conventional T2-weighted images. J. Neurol. 244, 266–270.

Song, S.K., Sun, S.W., Ju, W.K., Lin, S.J., Cross, A.H., Neufeld, A.H., 2003. Diffusion tensor imaging detects and differentiates axon and myelin degeneration in mouse optic nerve after retinal ischemia. Neuroimage 20, 1714–1722.

Song, S.K., Sun, S.W., Ramsbottom, M.J., Chang, C., Russell, J., Cross, A.H., 2002. Dysmyelination revealed through MRI as increased radial (but unchanged axial) diffusion of water. Neuroimage 17, 1429–1436.

Sotak, C.H., 2002. The role of diffusion tensor imaging in the evaluation of ischemic brain injury − a review. NMR Biomed. 15, 561–569.

Sullivan, E.V., Adalsteinsson, E., Pfefferbaum, A., 2006. Selective age-related degradation of anterior callosal fiber bundles quantified in vivo with fiber tracking. Cereb. Cortex 16, 1030–1039.

Sullivan, E.V., Pfefferbaum, A., Adalsteinsson, E., Swan, G.E., Carmelli, D., 2002. Differential rates of regional brain change in callosal and ventricular size: a 4-year longitudinal MRI study of elderly men. Cereb. Cortex 12, 438–445.

Sullivan, E.V., Rohlfing, T., Pfefferbaum, A., 2010. Quantitative fiber tracking of lateral and interhemispheric white matter systems in normal aging: relations to timed performance. Neurobiol. Aging 3, 464–481.

Terao, S., Sobue, G., Hashizume, Y., Shimada, N., Mitsuma, T., 1994. Age-related changes of the myelinated fibers in the human corticospinal tract: a quantitative analysis. Acta Neuropathol. 88, 137–142.

Vernooij, M.W., de Groot, M., van der Lugt, A., Ikram, M.A., Krestin, G.P., Hofman, A., Niessen, W.J., Breteler, M.M., 2008. White matter atrophy and lesion formation explain the loss of structural integrity of white matter in aging. Neuroimage 43, 470–477.

Wahlund, L.O., Barkhof, F., Fazekas, F., Bronge, L., Augustin, M., Sjogren, M., Wallin, A., Ader, H., Leys, D., Pantoni, L., Pasquier, F., Erkinjuntti, T., Scheltens, P., 2001. A new rating scale for age-related white matter changes applicable to MRI and CT. Stroke 32, 1318–1322.

Yakovlev, P.I., Lecours, A.R., 1967. The myelogenetic cycles of regional maturation of the brain, in: Minkowski, A., (Ed.), Regional Development of the Brain in Early Life. Blackwell Scientific, Oxford.

Zahr, N.M., Rohlfing, T., Pfefferbaum, A., Sullivan, E.V., 2009. Problem solving, working memory, and motor correlates of association and commissural fiber bundles in normal aging: a quantitative fiber tracking study. Neuroimage 44, 1050–1062.

Zhang, Y., Du, A.T., Hayasaka, S., Jahng, G.H., Hlavin, J., Zhan, W., Weiner, M.W., Schuff, N., 2008. Patterns of age-related water diffusion changes in human brain by concordance and discordance analysis. Neurobiol. Aging, doi:10.1016/j.neurobiolaging.2006.11.020.

References

Basser, P.J., Mattiello, J., leBihan, D., 1994. Estimation of the effective self-diffusion tensor from the NMR spin echo. J. Magn. Reson. B 103, 247–254.

Basser, P.J., Pierpaoli, C., 1996. Microstructural and physiological features of tissues elucidated by quantitative-diffusion-tensor MRI. J. Magn. Reson. B 111, 209–219.

Mazziotta, J., Toga, A., Evans, A., Fox, P., Lancaster, J., Zilles, K., Woods, R., Paus, T., Simpson, G., Pike, B., Holmes, C., Collins, L., Thompson, P., MacDonald, D., Iacoboni, M., Schormann, T., Amunts, K., Palomero-Gallagher, N., Geyer, S., Parsons, L., Narr, K., Kabani, N., Le Goualher, G., Boomsma, D., Cannon, T., Kawashima, R., Mazoyer, B., 2001. A probabilistic atlas and reference system for the human brain: International Consortium for Brain Mapping (ICBM). Philos. Trans. R. Soc. Lond. B Biol. Sci. 356, 1293–1322.

Pagani, E., Agosta, F., Rocca, M.A., Caputo, D., Filippi, M., 2008. Voxel-based analysis derived from fractional anisotropy images of white matter volume changes with aging. Neuroimage 41, 657–667.

Pagani, E., Filippi, M., Rocca, M.A., Horsfield, M.A., 2005. A method for obtaining tract-specific diffusion tensor MRI measurements in the presence of disease: application to patients with clinically isolated syndromes suggestive of multiple sclerosis. Neuroimage 26, 258–265.

Pagani, E., Horsfield, M.A., Rocca, M.A., Filippi, M., 2007. Assessing atrophy of the major white matter fiber bundles of the brain from diffusion tensor MRI data. Magn. Reson. Med. 58, 527–534.

Rohde, G.K., Aldroubi, A., Dawant, B.M., 2003. The adaptive bases algorithm for intensity-based nonrigid image registration. IEEE Trans. Med. Imaging 22, 1470–1479.

Studholme, C., Hill, D.L., Hawkes, D.J., 1997. Automated three-dimensional registration of magnetic resonance and positron emission tomography brain images by multiresolution optimization of voxel similarity measures. Med. Phys. 24, 25–35.